

Magnetic properties of gadolinium-doped β -tricalcium phosphate

Kouichi Nakashima^{a,*}, Jun Yamauchi^b

^a Graduate School of Human and Environmental Studies, Kyoto University, Japan

^b Graduate School of Science, Kyoto University, Japan

Received 31 July 2004; received in revised form 1 December 2004; accepted 1 December 2004

Available online 21 June 2005

Abstract

The frequency of radiant energy used in the majority of electron spin resonance (ESR) spectrometers is approximately 9 GHz (X-band), in the medium-frequency microwave region. Recently, high frequency microwave (Q-band) has been used to measure ESR spectra because high frequency ESR enhances the sensitivity. In the present work, ESR spectra (X-band, Q-band) of gadolinium-doped β -tricalcium phosphate (β -Ca₃(PO₄)₂:Gd, β -TCP:Gd) were investigated. X-band and Q-band ESR spectra were recorded. Q-band ESR spectra was observed clearer than X-band ESR spectra. The ESR spectra were assigned to the typical fine structure of the Gd³⁺ ion. The crystal-field parameters obtained at room temperature were determined to be $b_2^0 = -267.0$, $b_4^0 = -1.5$, and $b_6^0 = -6.4$ cm⁻¹.

© 2005 Elsevier B.V. All rights reserved.

Keywords: Electron spin resonance (ESR); β -Tricalcium phosphate (β -TCP); Gadolinium

1. Introduction

Much attention has been paid recently to ESR analysis of trivalent gadolinium ion (Gd³⁺) [1–4], which substitutes various compounds [5,6]. ESR is a powerful method to study the magnetic properties and crystal-field symmetry of rare earth compounds. In general, it is difficult to observe an ESR spectrum of trivalent rare earth ions at room temperature because of spin–orbit interaction and fast relaxation time. However, the Gd³⁺ ion permitted easy detection of the ESR spectrum even at room temperature.

The Gd³⁺ ion has seven electron spins on the 4f orbital (spin angular momentum $S = 7/2$, orbital angular momentum $L = 0$, total angular momentum $J = 7/2$) and the ground state of the Gd³⁺ ion is referred to ⁸S_{7/2}. ESR spectroscopy is suitable for measuring the above-mentioned electron spins.

In this investigation, magnetic properties about crystal-field parameters of the Gd³⁺ ion were examined using ESR spectroscopy. The zero-field splitting of the Gd³⁺ ion is gener-

ally as large as the X-band microwave energy. In the Q-band ESR measurements, the Zeeman term dominates the zero-field splitting in the spin Hamiltonian, and the spectrum exhibits a pattern that can be easily assigned [7,8]. The combined use of a X- and Q-band spectroscopy makes the analysis simple and reliable.

2. Experimental methods

2.1. Sample preparation

Gadolinium-doped amorphous calcium phosphate (Ca₃(PO₄)₂·*n*H₂O:Gd, ACP:Gd) as a starting material [9] was prepared at 0 °C by rapid addition, with stirring, of a 0.100 mol dm⁻³ diammonium hydrogen phosphate ((NH₄)₂HPO₄) solution to a 0.167 mol dm⁻³ calcium nitrate (Ca(NO₃)₂) solution containing gadolinium nitrate; the pH of the suspension turned out to be 10.00. The pH of the (NH₄)₂HPO₄ solution was adjusted to 10.48 with concentrated aqueous ammonia (NH₄OH) prior to mixing, and the reaction was carried out in a closed system to reduce carbon dioxide (CO₂) contamination. The initial solid phase, formed

* Corresponding author. Tel.: +81 75 753 2888; fax: +81 75 753 6694.

E-mail address: kouichi@yamauchi.mbox.media.kyoto-u.ac.jp (K. Nakashima).

immediately on mixing, was separated from the mother liquor by filtration and washed with cold ammoniated water at pH 10.00. It was then dried with cold acetone and dry air. β -TCP:Gd was prepared by a heat treatment of ACP:Gd at 1100 °C in an electric furnace (FP21, Yamato Scientific Co. Ltd.) in air for 2 h and then gradually cooled to room temperature. Incidentally, a platinum crucible was used for the heat treatment of ACP:Gd. The elemental compositions of β -TCP:Gd were determined with an ICP emission spectrometer (SPS1200A, Seiko Instruments Inc. Co. Ltd.).

2.2. Characterization

Powder X-ray diffraction patterns of β -TCP and β -TCP:Gd were measured with an X-ray diffractometer (XRD-6000, Shimadzu Co. Ltd. 40 kV, 30 mA) using Cu K α radiation with a wavelength of 0.15406 nm at room temperature.

ESR measurements were carried out on β -TCP:Gd. The ESR spectra were recorded equipped with a 100 kHz magnetic-field modulation (X-band: JES-RE3X (JEOL Co. Ltd.), Q-band: JES-FE3X (JEOL Co., Ltd.)). The ESR microwave power was low enough to avoid the saturation and the distortion of the spectrum.

3. Structure of β -Ca₃(PO₄)₂:Gd

The powder X-ray diffraction pattern of β -TCP:Gd is shown in Fig. 1. β -TCP has the rhombohedral space group $R3c$ with unit cell $a=b=1.0439$ nm and $c=3.7375$ nm (hexagonal setting) with 21 formula units per hexagonal unit cell [10,11]. The single phase of β -TCP:Gd was obtained at the Gd/Ca atomic ratio 8×10^{-3} .

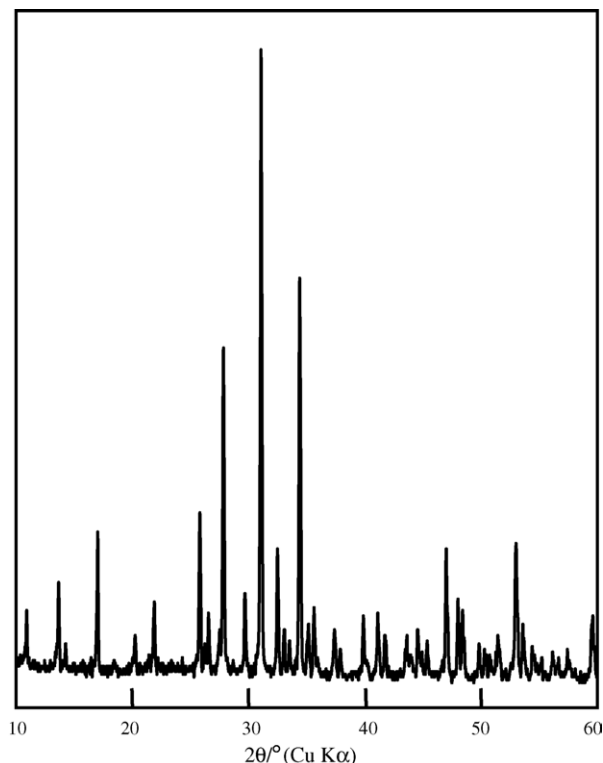


Fig. 1. Powder X-ray pattern of β -Ca₃(PO₄)₂:Gd.

Structure of β -TCP:Gd [12,13] is illustrated in Fig. 2. In this description, emphasis is given to columns of ions of the form $\cdots\text{PO}_4 \text{ Ca Ca Ca PO}_4 \cdots$ that can be identified running parallel to the c -axis. The Gd³⁺ ion is generally substituted for Ca (4) site in A column.

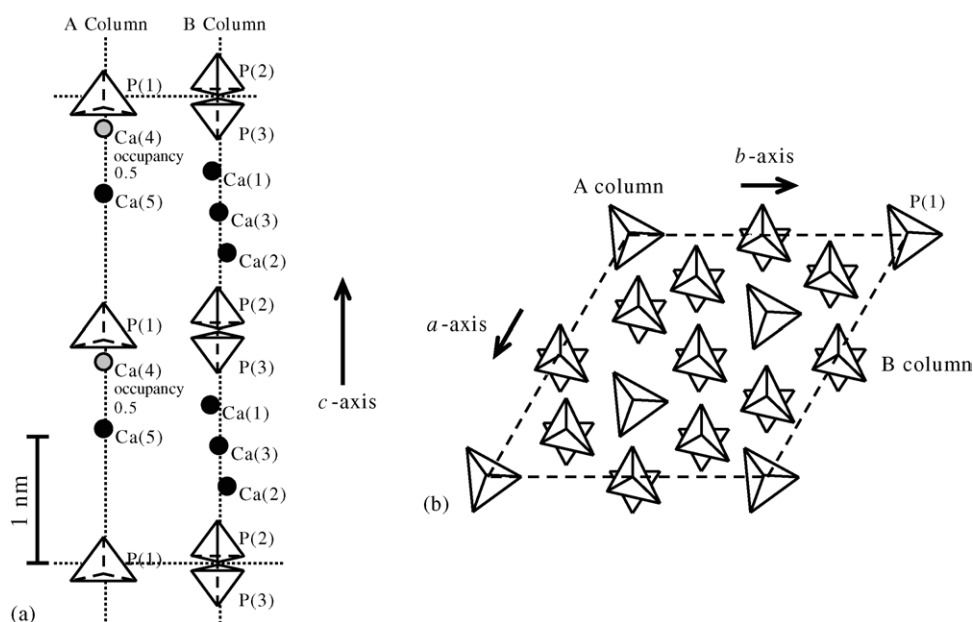


Fig. 2. Structure of β -Ca₃(PO₄)₂.

4. Results and discussion

4.1. Spin Hamiltonian of Gd^{3+} ion

For the Gd^{3+} ion with $^8S_{7/2}$ ground state, fine-structure ESR spectra can be analyzed in terms of the following spin Hamiltonian [7]:

$$H = H_{eZ} + H_{FS} = \mu_B \mathbf{H} \cdot \mathbf{g} \cdot \mathbf{S} + \sum_{k,q} B_k^q O_k^q, \\ k, q = 2, 4, 6 \text{ and } k \geq q = \mu_B \mathbf{H} \cdot \mathbf{g} \cdot \mathbf{S} + \frac{1}{3}(b_2^0 O_2^0 + b_2^2 O_2^2) \\ + \frac{1}{60}(b_4^0 O_4^0 + b_4^2 O_4^2 + b_4^4 O_4^4) \\ + \frac{1}{1260}(b_6^0 O_6^0 + b_6^2 O_6^2 + b_6^4 O_6^4 + b_6^6 O_6^6) \quad (1)$$

where $b_2^q = 3B_2^q$, $b_4^q = 60B_4^q$, $b_6^q = 1260B_6^q$, $D = b_2^0$, and $E = (b_2^2/3)$ (D and E are zero-field splitting constants).

The spin Hamiltonian used to describe the powder spectra has been assumed to have second-order crystal-field which are much larger than the high order terms, but which are much smaller than the Zeeman interaction. The addition of small higher order crystal-field terms to this Hamiltonian may change the position but not the identification of the extremes. The described by Eq. (1) are given to second order by

$$\left(\mp \frac{7}{2}\right) \leftrightarrow \left(\pm \frac{5}{2}\right), \\ H = \frac{1}{g\mu_B} \left\{ h\nu \mp (6b_2^0 + 20b_4^0 + 6b_6^0) \right. \\ \left. + E' \left(\frac{45}{1 \pm 3F} - \frac{21}{1 \pm 5F} \right) \right\}, \\ \left(\pm \frac{5}{2}\right) \leftrightarrow \left(\pm \frac{3}{2}\right), \\ H = \frac{1}{g\mu_B} \left\{ h\nu \mp (4b_2^0 - 10b_4^0 - 14b_6^0) \right. \\ \left. + E' \left(\frac{60}{1 \pm F} - \frac{21}{1 \pm 5F} - \frac{45}{1 \pm 3F} \right) \right\}, \\ \left(\pm \frac{3}{2}\right) \leftrightarrow \left(\pm \frac{1}{2}\right), \\ H = \frac{1}{g\mu_B} \left\{ h\nu \mp (2b_2^0 - 12b_4^0 - 14b_6^0) \right. \\ \left. + E' \left(\frac{21}{1 \pm 5F} - \frac{45}{1 \pm 3F} \right) \pm E'^2 \left(\frac{120F}{1 - F^2} \right) \right\}, \\ \left(+\frac{1}{2}\right) \leftrightarrow \left(-\frac{1}{2}\right), \\ H = \frac{1}{g\mu_B} \left\{ h\nu \pm E' \left(\frac{90}{1 - 9F^2} - \frac{120}{1 - F^2} \right) \right\} \quad (2)$$

where $E' = \frac{(b_2^2)^2}{18g\mu_B H}$ and $F = \frac{b_2^0}{g\mu_B H}$. Taking differences between the three functionally similar pairs of transitions denoted by $M_s \leftrightarrow M_s - 1$ and $-M_s + 1 \leftrightarrow -M_s$, one eliminates much of the second-order correction and obtains

$$H \left(+\frac{7}{2} \leftrightarrow +\frac{5}{2} \right) - H \left(-\frac{5}{2} \leftrightarrow -\frac{7}{2} \right) \\ = -\frac{1}{g\mu_B} (12b_2^0 + 40b_4^0 + 12b_6^0), \\ H \left(+\frac{5}{2} \leftrightarrow +\frac{3}{2} \right) - H \left(-\frac{3}{2} \leftrightarrow -\frac{5}{2} \right) \\ = -\frac{1}{g\mu_B} (8b_2^0 - 20b_4^0 - 28b_6^0), \\ H \left(+\frac{3}{2} \leftrightarrow +\frac{1}{2} \right) - H \left(-\frac{1}{2} \leftrightarrow -\frac{3}{2} \right) \\ = -\frac{1}{g\mu_B} (4b_2^0 - 24b_4^0 + 28b_6^0) \quad (3)$$

where terms of the order of E' and F are omitted. These equations may be used to determine b_2^0 , b_4^0 , and b_6^0 . For $H \perp z$ corresponding equations can be derived from the transformation properties of the O_n^m operators [7]. They are to first order

$$H \left(+\frac{7}{2} \leftrightarrow +\frac{5}{2} \right) - H \left(-\frac{5}{2} \leftrightarrow -\frac{7}{2} \right) \\ = \frac{1}{g\mu_B} \left(6b_2^0 - 15b_4^0 + \frac{15}{4}b_6^0 - 6b_2^2 \cos 2\phi \right. \\ \left. - 5b_4^4 \cos 4\phi \right), \\ H \left(+\frac{5}{2} \leftrightarrow +\frac{3}{2} \right) - H \left(-\frac{3}{2} \leftrightarrow -\frac{5}{2} \right) \\ = \frac{1}{g\mu_B} \left(4b_2^0 + \frac{15}{2}b_4^0 - \frac{35}{4}b_6^0 - 4b_2^2 \cos 2\phi \right. \\ \left. + \frac{5}{2}b_4^4 \cos 4\phi \right), \quad b_2^0, \\ H \left(+\frac{3}{2} \leftrightarrow +\frac{1}{2} \right) - H \left(-\frac{1}{2} \leftrightarrow -\frac{3}{2} \right) \\ = \frac{1}{g\mu_B} \left(2b_2^0 + 9b_4^0 + \frac{35}{4}b_6^0 - 2b_2^2 \cos 2\phi \right. \\ \left. + 3b_4^4 \cos 4\phi \right) \quad (4)$$

where ϕ is the angle between the magnetic field and the x -axis. Any pair of Eq. (4) can be solved for the two remaining unknowns b_2^0 and b_4^0 .

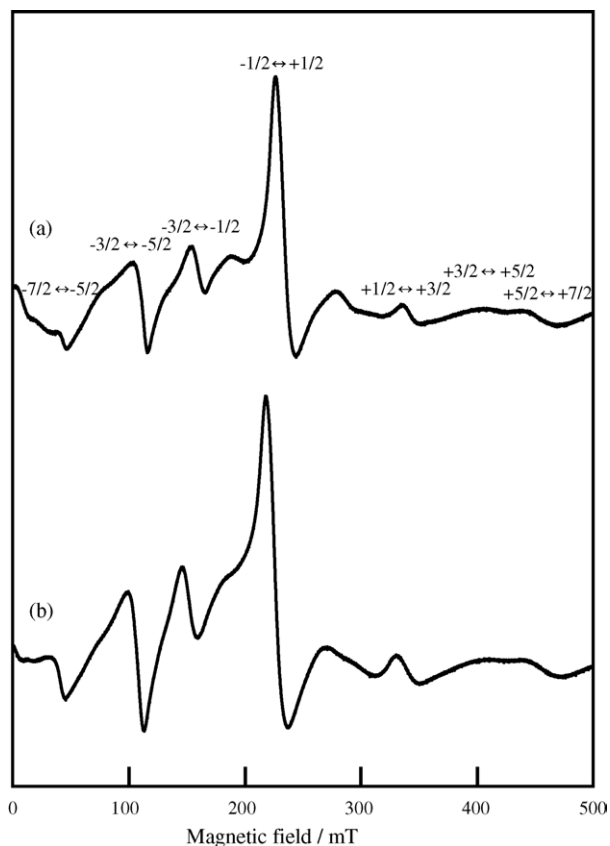


Fig. 3. X-band ESR spectra of $\beta\text{-Ca}_3(\text{PO}_4)_2\text{:Gd}$. Frequency, (a) 9.432 GHz, (b) 9.194 GHz, modulation: 0.2×1 mT, amplitude, (a) 1×10 , (b) 5×1 , temperature (K) (a) room temperature, (b) 120 K.

4.2. X- and Q-band ESR spectra of $\beta\text{-Ca}_3(\text{PO}_4)_2\text{:Gd}$

It is well-known that crystalline electric field interact weakly with the $^8\text{S}_{7/2}$ ground state of the Gd^{3+} ion. The crystal-field splitting for the Gd^{3+} ion is generally smaller than that produced by the Zeeman interaction in the X-band ESR experiments, and for the Gd^{3+} ions in most hosts, all the resulting levels are appreciably populated at temperatures above 4 K. The ESR spectrum generally consists of seven anisotropic lines described by a spin Hamiltonian incorporating both crystal-field and Zeeman operators.

In observations made at X-band from room temperature to 4 K, the ESR spectrum was found to consist of a single set of seven lines. At Q-band ESR measurement from room temperature to 120 K, the ESR spectra could be observed. X- and Q-band ESR spectra of the Gd^{3+} ion were investigated at both room temperature and 120 K (Figs. 3 and 4). Consideration from the previous reports, the component of the z-axis was observed in the present ESR spectra, mainly [13]. ESR signal intensity of both X- and Q-band spectra at 120 K were stronger than room temperature because of the population difference. ESR intensity is proportional to the population difference of the two states which is involved in the transitions [14]. This is given by the Boltzmann distribution [15]. These ESR spectra were assigned to the typical fine structure

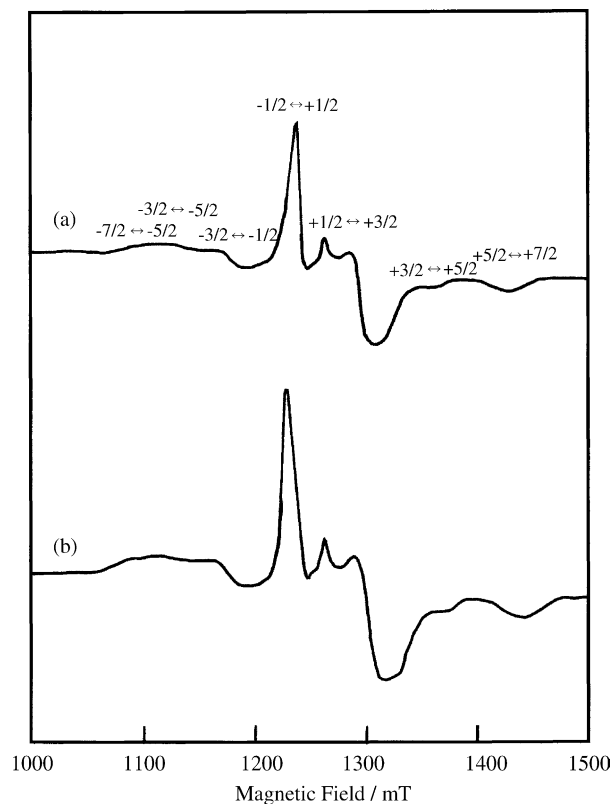


Fig. 4. Q-band ESR spectra of $\beta\text{-Ca}_3(\text{PO}_4)_2\text{:Gd}$. Frequency, (a) 35.1293 GHz, (b) 35.2078 GHz, modulation: 0.2×1 mT, amplitude, (a): 2×100 , (b): 1×100 , temperature (K), (a) room temperature, (b) 120 K.

Table 1

Observed spin Hamiltonian parameters for Gd^{3+} ion in $\beta\text{-Ca}_3(\text{PO}_4)_2\text{:Gd}$

	Room temperature	120 K
b_2^0	-267.0	-287.1
b_4^0	-1.5	1.6
b_6^0	6.4	2.5

All crystal-field parameters are given in units of 10^{-4} cm^{-1} . Q-band ESR measurement.

of the Gd^{3+} ion. The transitions and magnetic field values for the ESR line positions were determined. These values leads to the crystal-field parameters of b_2^0 , b_4^0 , and b_6^0 from the calculations on condition that Landé-g-factor = 2 of the Gd^{3+} ion [16]. The crystal-field parameters are listed in Table 1. Compared with the previous reports [5,7,8], the crystal-field parameters of Gd^{3+} in b-TCP:Gd are small.

5. Conclusions

The magnetic properties about crystal-field parameters for $\beta\text{-TCP:Gd}$ were examined in terms of X- and Q-band ESR spectroscopy. The X-band ESR spectra exhibit the fine-structure consisting of seven lines due to the Gd^{3+} ion. Q-band ESR spectra was observed clearer than X-band ESR spectra. Recording the powder ESR patterns of the Gd^{3+} ion,

spin Hamiltonian of the Gd^{3+} ion was determined from the spectral analysis including higher order fine-structure parameters. Concluding the research, the values of the crystal-field parameters and zero-field splitting constants could be estimated.

Acknowledgements

The authors would like to express their appreciation to Dr. Masaaki Baba (Kyoto University, Japan) for his various discussions.

References

- [1] V.A. Atsarkin, V.V. Demidov, G.A. Vasneva, B.M. Odintsov, R.L. Belford, B. Radüchel, R.B. Clarkson, *J. Phys. Chem. A* 105 (2001) 9323–9327.
- [2] A. Borel, F. Yerly, L. Helm, A. Merbach, *J. Am. Chem. Soc.* 124 (2002) 2042–2048.
- [3] S. Rast, A. Borel, L. Helm, E. Belorizky, P.H. Fries, A.E. Merbach, *J. Chem. Phys.* 123 (2001) 2637–2644.
- [4] N. Ishikawa, N. Tanaka, Y. Kaizu, *Inorg. Chim. Acta* 357 (2004) 2181–2184.
- [5] V.A. Ivanshin, G.V. Mamin, A. Shengelaya, H. Keller, P.W. Klamut, A. Sikora, *Solid State Commun.* 110 (1999) 147–152.
- [6] D. Zayachuk, Y. Polyhach, E. Slynko, O. Khandozhko, C. Rudowicz, *Physica B* 322 (2002) 270–275.
- [7] R.W. Reynolds, L.A. Boatner, C.B. Finch, A. Chatelain, M.M. Abraham, *J. Chem. Phys.* 56 (1972) 5607–5625.
- [8] K. Furukawa, S. Okubo, H. Kato, H. Shinohara, T. Kato, *J. Am. Chem. Soc.* 107 (2003) 10933–10937.
- [9] K. Nakashima, M. Takami, M. Ohta, Y. Iima, J. Yamauchi, *Adv. ESR Appl.* 20 (2003) 3–6.
- [10] T. Toyama, K. Nakashima, T. Yasue, *J. Ceram. Soc. Jpn.* 110 (2002) 716–721.
- [11] B. Dickens, L.W. Schroeder, W.E. Brown, *J. Solid State Chem.* 10 (1974) 232–248.
- [12] J.C. Elliott, *Structure and Chemistry of the Apatites and Other Calcium Phosphate*, Elsevier, London, 1994, pp. 37–40.
- [13] C.A. Baumann, R.J. Van Zee, K.J. Zeringue, W. Weltner Jr., *J. Chem. Phys.* 75 (1981) 5291–5296.
- [14] J.A. Weil, J.R. Bolton, J.E. Wertz, *Electron Paramagnetic Resonance, Elementary Theory and Practical Applications*, 1994, pp. 93–94.
- [15] J.A. Weil, J.R. Bolton, J.E. Wertz, *Electron Paramagnetic Resonance, Elementary Theory and Practical Applications*, 1994, pp. 287–294.
- [16] J.A. Weil, J.R. Bolton, J.E. Wertz, *Electron Paramagnetic Resonance, Elementary Theory and Practical Applications*, 1994, pp. 197–212.